

COMPUTER CALCULATION OF THE PHASE DIAGRAMS OF SILICATE SYSTEMS

MAREK LIŠKA, VLADIMÍR DANĚK*

Joint Laboratory of Centre of Chemical Research, Slovak Academy of Sciences, and of Glass Research and Development Institute, Trenčín, CS — 912 50

**Institute of Inorganic Chemistry, Centre of Chemical Research, Slovak Academy of Sciences, Bratislava, CS — 842 36*

Received 22. 6. 1989

A general algorithm and a FORTRAN program for the calculation of isobaric phase diagrams of polymeric oxide systems based on the thermodynamic model of silicate melts was developed. This software enables the primary crystallization temperatures for a single configuration point to be determined and the phase diagrams for a binary or ternary systems to be constructed.

The verification of the computational algorithm was demonstrated on simple ternary eutectic systems, a pseudoternary system with four crystallization phases and a ternary system in which some binary and ternary compounds are formed.

The way of using this method in structural studies of silicate melts was described.

INTRODUCTION

In the past decades, the theoretical calculations of phase diagrams have become an efficient research tool in several fields of science and engineering. This fact is a result of the effective employment of both computer techniques and fundamental principles of chemical thermodynamics. The attractiveness and need of such calculations have also been testified by an unceasingly rising number of papers, reviews and monographs [1—5]. Interesting practical application of theoretical calculations of phase diagrams for silicate systems were reported in [6]. Applying the simplified LeChatelier-Schreder equation to binary and pseudobinary systems, the authors of the work cited calculated coordinates of eutectic points and by means of the Prigogine equation [7] determined phase separation regions in ternary systems. The main aim of the work [6] was to utilize calculated results in the development of new special types of glasses with required properties.

Each theoretical calculation of solid-liquid phase equilibria is based on the choice of a suitable thermodynamic model for the liquid phase which also sufficiently considers the structural aspects. Owing to the polymeric character of silicate melts, the classic regular solution approach is not applicable, because limiting laws are not obeyed when the Clausius-Clapeyron equation is used. Temkin's model of an ideal ionic solution which has been widely employed in molten salt systems, was not found suitable for silicates, as their real anionic composition, owing to a broad polyanionic distribution, is not known a priori.

The optimum approach to the calculation of activity of individual components in silicate systems was published in [8—11] and applied to various types of silicate borate and aluminosilicate systems. The model is based on the definition of chemical potentials of all the atoms. Different energy and consequently structural states of the atoms are considered. In the present work a general algorithm for isobaric phase diagrams of polymeric oxide systems was developed. The program is written in FORTRAN and provides an interactive service with graphic output.

THEORETICAL

Let us consider an arbitrary mixture in the MeO—SiO₂ system (Me = Mg, Ca, ...). The melt of such a mixture is composed of the following types of atoms Me²⁺ cations, silicon atoms in tetrahedral coordination with oxygens, and two kinds of oxygen atoms — the bridging ones connecting two neighbouring SiO₄ tetrahedra by means of Si—O—Si covalent bonds, and the non-bridging ones bound to one silicon atom only and creating the coordination sphere of Me²⁺ cations. Evidently, the two types of oxygen atoms are distinguishable by their energies and their mutual molar ratio defines the structure of a melt, that is its polymerization degree as well as the chemical potentials of its components. With regard to this structural aspect of silicate systems, the chemical potential of an arbitrary component may be defined as a sum of chemical potentials of all atoms forming the component considered, as their particular energy states are taken into account. The chemical potential of the *i*-th component in a solution is defined as

$$\mu_i = \sum_j \mu_j n_{i,j}, \quad (1)$$

where $n_{i,j}$ is the amount of atoms of the *j*-th type in the *i*-th component and μ_j is the chemical potential of atoms of the *j*-th type in the solution. For instance, the chemical potential of CaSiO₃, which is formed in the CaO—SiO₂ system, equals to the sum of the chemical potentials of calcium atoms, silicon atoms, and the bridging and non-bridging oxygen atoms. The activity of the *i*-th component in a solution also obeys the equation

$$\mu_i = \mu_i^\circ + RT \ln a_i \quad (2)$$

where μ_i° is the chemical potential of the pure *i*-th component, defined similarly to the chemical potential of this component in a solution

$$\mu_i^\circ = \sum_j \mu_{i,j}^\circ n_{i,j}, \quad (3)$$

where $\mu_{i,j}^\circ$ is the chemical potential of the *j*-th atoms in the pure *i*-th component. Substituting eqns (1) and (3) into eqn (2) we obtain

$$\sum_j \mu_j n_{i,j} = \sum_j \mu_{i,j}^\circ n_{i,j} + RT \ln a_i. \quad (4)$$

The real mole fractions of the *j*-th atoms in the pure *i*-th component and in the solution are given by

$$y_{i,j}^\circ = \frac{n_{i,j}}{\sum_j n_{i,j}} \quad (5)$$

$$y_j = \frac{\sum_i n_{i,j} x_i}{\sum_i x_i \sum_j n_{i,j}} \quad (6)$$

where x_i is the molar fraction of the *i*-th component in the solution. The chemical potentials of the *j*-th atoms in the pure *i*-th component and in the solution may also be expressed using eqns (5) and (6) in following way

$$\mu_{i,j}^\circ = \mu_j^\dagger + RT \ln y_{i,j}^\circ \quad (7)$$

$$\mu_j = \mu_j^\dagger + RT \ln y_j, \quad (8)$$

where μ_j^\dagger is the chemical potential of a hypothetical liquid composed exclusively of the j -th atoms. Substitution of eqns (7) and (8) into eqn (4) gives for the activity of the i -th component in the solution the relation

$$\ln a_i = \sum_j n_{i,j} \ln y_j - \sum_j n_{i,j} \ln y_{i,j}^\circ, \quad (9)$$

or after rearrangement

$$a_i = \prod_j \left(\frac{y_j}{y_{i,j}^\circ} \right)^{n_{i,j}} \quad (10)$$

Eqn (10) for the activity of a component derived in this way is wholly universal and may be used in any system. The calculation of the activity of a component in an actual system according to this equation thus respects some structural aspects, e.g. different energy states of atoms of the same type. Such cases may occur in the presence of tri-valent atoms like B^{3+} , Al^{3+} , Fe^{3+} , etc.

Let us assume that in a system consisting of m oxides the polymeric network is formed by three- and four-fold coordinated atoms jA ($j = 1, 2, \dots, m$) bound to bridging (0°) and non-bridging (0^-) oxygen atoms. Designating the fraction of k -fold co-ordinated jA atoms as $\alpha_{k,j}$, the following inequality has to be obeyed

$$\alpha_{3,j} + \alpha_{4,j} \leq 1. \quad (11)$$

The distribution of the atoms according to their co-ordination or to their participation in a covalent network, is then determined by the material balance

$$n(^jA) = n_0(^jA) + n_3(^jA) + n_4(^jA) \quad (12)$$

where

$$n_0(^jA) = (1 - \alpha_{3,j} - \alpha_{4,j}) n(^jA), \quad (13)$$

$$n_3(^jA) = \alpha_{3,j} n(^jA), \quad (14)$$

$$n_4(^jA) = \alpha_{4,j} n(^jA), \quad (15)$$

where $n_k(^jA)$ indicates the amount of the k -fold co-ordinated jA atoms and $n_0(^jA)$ the amount of those jA atoms which are not built into the polyanionic network. Assuming the total amount of oxygen $n(0)$ is divided between bridging and non-bridging oxygen atoms, we can find their amounts $n(0^\circ)$ and $n(0^-)$ from the material balances of the amounts of oxygen and jA -O bonds

$$n(0) = n(0^\circ) + n(0^-) \quad (16)$$

$$n(0^-) + 2n(0^\circ) = \sum_{j=1}^m [n(^jA) (3\alpha_{3,j} + 4\alpha_{4,j})]. \quad (17)$$

If the solution of this system makes no physical sense (i.e. the values of n are negative) it is necessary to assume that oxygen atoms are present as non-bridging ones and as oxygen ions O^{2-} . Then the material balance is represented by the following equations

$$2 \cdot n(0^-) = \sum_{j=1}^m [n(^jA) (3\alpha_{3,j} + 4\alpha_{4,j})] \quad (18)$$

$$n(O^{2-}) = n(0) - n(0^-). \quad (19)$$

Typical modifying atoms such as alkali metals and alkaline earth metals are assumed to give

$$\alpha_{3,j} = \alpha_{4,j} = 0, \quad (20)$$

while typical network forming elements of the IV-th group of the periodic system like silicon and germanium give

$$\alpha_{3,j} = 0 \quad \text{and} \quad \alpha_{4,j} = 1. \quad (21)$$

In other cases the values of α can be determined by fitting the calculated phase diagrams to those determined experimentally.

According to eqns (16) and (17), the formal polymerization degree P of a system with a known composition can be determined. Since the polymerization degree is defined as the ratio of the amount of bridging oxygen atoms to the total amount of oxygen, one can write

$$P = \frac{n(0^\circ)}{n(0)} = \frac{\sum_{j=1}^m [n(jA) (3\alpha_{3,j} + 4\alpha_{4,j})]}{n(0)} - 1. \quad (22)$$

For instance, in the $(1-x) \cdot \text{MeO} + x \text{SiO}_2$ mixture $m = 2$, ${}^1A = \text{Me}$, ${}^2A = \text{Si}$, $\alpha_{3,1} = \alpha_{3,2} = \alpha_{4,1} = 0$ and $\alpha_{4,2} = 1$. Then

$$P = \frac{4x}{1+x} - 1. \quad (23)$$

In such a mixture, $P = 0$ for $x = 1/3$, i.e. for the composition of orthosilicate, and $P = 1$ for the pure SiO_2 melt.

The calculation of liquidus temperatures for the individual components $T_{i,\text{liq}}$ is performed using corresponding experimental values of enthalpy and temperature of fusion according to the simplified and adapted LeChatelier-Schreder equation

$$T_{i,\text{liq}} = \frac{\Delta H_{f,i} T_{f,i}}{\Delta H_{f,i} - RT_{f,i} \ln a_i} \quad (24)$$

where $T_{f,i}$ and $\Delta H_{f,i}$ are the temperature and enthalpy of fusion of the i -th component, respectively, and a_i is its activity calculated according to eqn (10). The primary crystallization temperature of the melt with a known composition is then determined as the maximum liquidus temperature of all the components in question

$$T_{pc} = \max_i (T_{i,\text{liq}}). \quad (25)$$

THE CALCULATION ALGORITHM

Actually it is impossible to resolve the problem described without an efficient computer. The aim of this work was to elaborate a general algorithm and program for solid liquid phase equilibria calculations in various types of polymeric oxide systems. An adequately general set of input makes it possible to work in diverse compositional spaces comprising several, up to ten, oxides, thus providing a wide field of application for the program. The sub-space in which the phase diagram is constructed, can be non-, one- or two-dimensional (a point, a line or a plane),

respectively, and can be defined either by the composition of the respective phases, or by the coordinates of the chosen compositional space. Each cation may participate in a polymeric network in three- and/or four-fold coordination and this fact can be specified. The program is divided into several subroutines, so that modification of an arbitrary part of the algorithm presents no special difficulties. The structure of the main program FADR is presented in form of a program flowchart in Fig. 1. The relations between the individual subroutines are shown in Fig. 2.

Subroutine INPUT starts the calculation and provides stoichiometric description of an actual oxide system A_xO_y , $j = 1, 2, \dots, m$ which comprises the compositional space, and input of $\alpha_{3,j}$ and $\alpha_{4,j}$ for all the A atoms. The data can be entered via a keyboard or from an appropriate file. Chemical elements are specified directly by their chemical symbols. Molar masses of oxides are calculated automatically

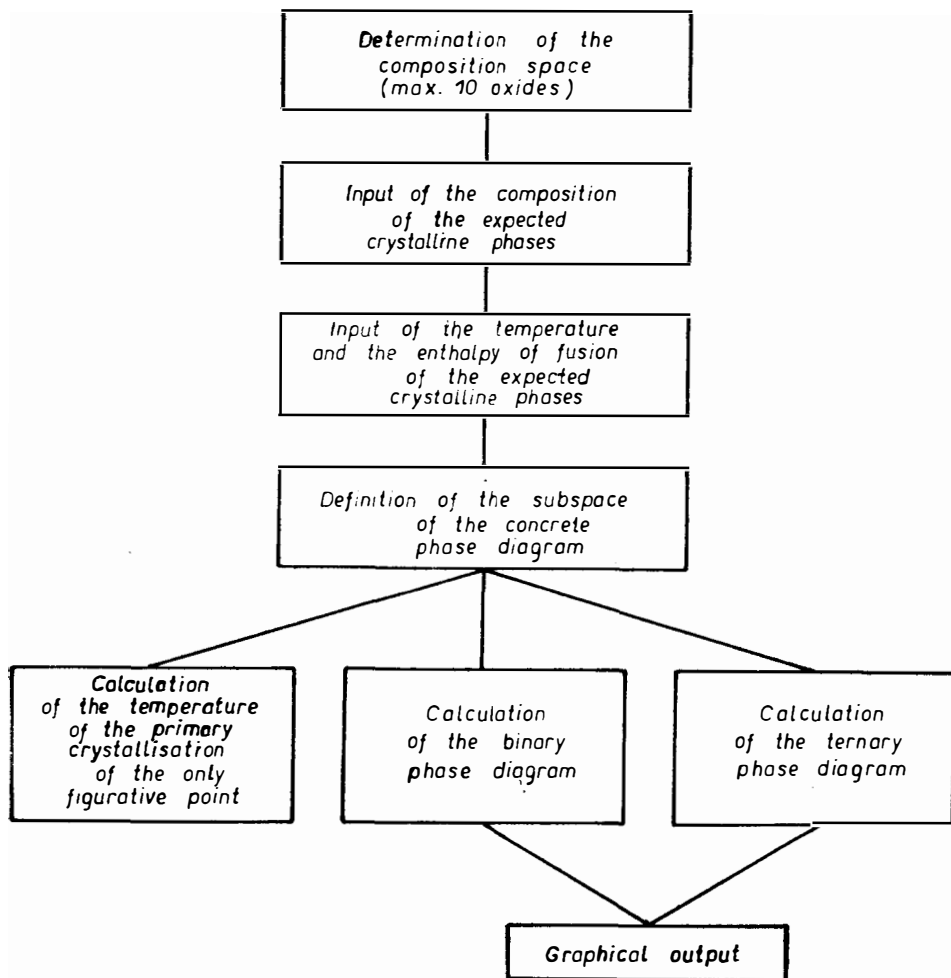


Fig. 1. Flowchart of the FADR program.

from atomic mass data stored in the memory. The next step is the input of the stoichiometric composition and the values of $\Delta H_{f,i}$ a $T_{f,i}$ for all the crystalline phases being expected to crystallize in the compositional space considered. After that the subroutine YCFR is called, which calculates the mole fractions $y_{i,j}^0$ of all the atom types (i.e. atoms A , bridging and non-bridging oxygen atoms) present in the crystalline phases. Then the control is returned back to the main program.

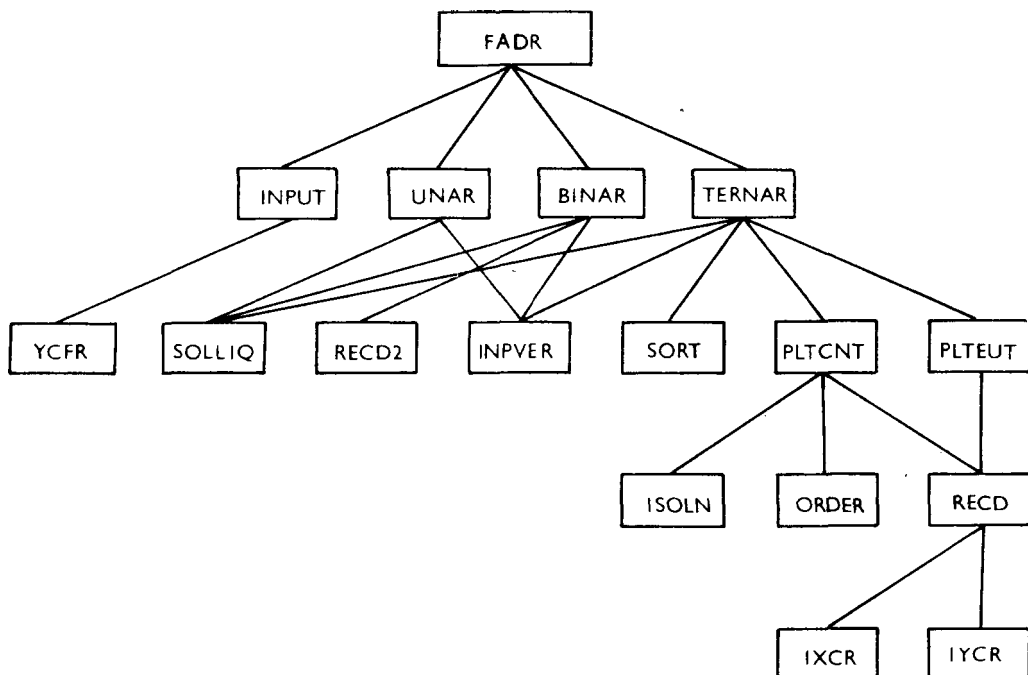


Fig. 2. Relations between individual subroutines in the FADR program.

The structure of the main program allows further direction of calculation to be chosen and proceeds with

- (i) determination of the primary crystallization temperature for a single compositional point of the system defined (subroutine UNAR);
- (ii) construction of the phase diagram for a binary system defined by two arbitrary points of the compositional space (subroutine BINAR);
- (iii) construction of the phase diagram for an arbitrary ternary system defined by three non-colinear points of the compositional space (subroutine TERNAR).

The graphic output of phase diagrams may be chosen in coordinates of either mole or mass fractions.

- (i) Calculation of the primary crystallization temperature for a single point in a compositional space

At first, the subroutine UNAR transfers control to subroutine INPVER, which ensures entering of compositions for one, two or three points from the compositional space according to the input parameters. Then control is transferred to subroutine

SOLLIQ which calculates the liquidus temperatures of all crystalline phases present and the primary crystallization temperature for a considered point of the compositional space.

(ii) Calculation of a binary phase diagram

Subroutine BINAR similarly to UNAR, calls at first the subroutine INPVER and two points of the compositional space determining a pseudobinary system are put in. Then follows the input of the upper and lower temperature limits for the temperature axis and the concentration axis division. With the help of subroutine SOLLIQ the primary crystallization temperatures for all concentration points (determined by the concentration axis division) are calculated and marked into the diagram. The positions of eutectic points are obtained by linear interpolation between two neighbouring concentration points differing in their respective primary crystallizing phases. The graphic output is provided by subroutine RECD2 processing the data set stored in a specified file. Owing to the software and hardware possibilities this data set can be used in different ways. In our case the graphic output was screened, and subsequently transferred to the printer to get a hard copy.

(iii) The calculation of a ternary phase diagram

A sophisticated algorithm was developed to calculate and draw ternary phase diagrams. Subroutine TERNAR first determines, by means of subroutine INPVER, the coordinates of the concentration triangle apices in the compositional space. Though in general this triangle is not equilateral in a chosen compositional space, the phase diagram is drawn as usually in an equilateral triangle. A rhombohedral network is first constructed in this triangle. Its density is determined by an input parameter. For the nodal points of this network the primary crystallization temperatures are calculated and line after line stored in the data file. To draw the isotherms of primary crystallization, couples of neighbouring lines are successively transferred to the operation memory. The direction of the respective isotherm is found in each rhombus using linear interpolation on the sides of the two triangles.

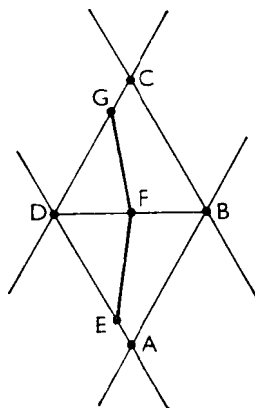


Fig. 3. Drawing of isotherms in the rhombohedral network.

formed by the rhombus diagonal. An elementary ABCD rhombus is shown in Fig. 3. The isotherm is drawn in two steps. First, line EF in the ABD triangle and after that line FG in the second triangle BCD are found. Subroutine PLTCNT with the help of ISOLN, ORDER, and RECD performs the drawing of the isotherms. Subroutine RECD writes down the data into the graphical instruction data set, and recalculation of mole or mass fraction co-ordinates to cartesian is performed by subroutines IXCR and IYCR.

The boundary lines between two neighbouring crystallization areas belonging to different crystalline phases are looked for during primary crystallization temperature calculations for nodal points of the rhombohedral network. If another crystallizing phase occurs while passing from one nodal point to the neighbouring one, then the co-ordinates of the point in which these phases have the same temperature $T_{i, liq}$, are determined by linear interpolation. These data are ordered by subroutine SORT so that the points belonging to the same boundary line are put to a sequence and the line is drawn by subroutine PLTEUT. Using a sufficiently dense network, this method gives directly ternary eutectic points as common points of three boundary lines.

RESULTS OF CALCULATION AND DISCUSSION

Three types of ternary and pseudoternary systems were considered to demonstrate the algorithm proposed:

- i) simple eutectic systems;
- ii) system with four crystallization areas where the figurative point of the fourth crystalline phase lies beyond the pseudoternary diagram;
- iii) a system where some binary and ternary compounds are formed.

Table I
Thermodynamic data of the individual compounds used
in the calculations

Compound	$\frac{T_f}{K}$	$\frac{\Delta H_f}{\text{kJ mol}^{-1}}$
CaO	2843	52.0
Al ₂ O ₃	2293	111.4
SiO ₂	1996	9.6
CaO . SiO ₂	1817	56.0
CaO . Al ₂ O ₃ . 2 SiO ₂	1826	166.8
2 CaO . Al ₂ O ₃ . SiO ₂	1868	155.9
2 CaO . SiO ₂	2403	55.4
3 CaO . 2 SiO ₂	1718	146.5
CaO . Al ₂ O ₃	1878	102.5
12 CaO . 7 Al ₂ O ₃	1728	209.3
3 Al ₂ O ₃ . 2 SiO ₂	2123	188.3
MnO . SiO ₂	1564	66.9
MgO . Al ₂ O ₃	2408	200.0
MgO . SiO ₂	1850	75.2
CaO . MgO . 2 SiO ₂	1665	128.3
CaO . 2 Al ₂ O ₃	2033	200.0

The systems $\text{CaO} \cdot \text{MgO} \cdot 2 \text{SiO}_2$ (CMS_2)— $\text{MnO} \cdot \text{SiO}_2$ ($\overline{\text{MS}}$)— $\text{CaO} \cdot \text{Al}_2\text{O}_3 \cdot 2 \text{SiO}_2$ (CAS_2), $\text{MgO} \cdot \text{SiO}_2$ (MS)— CMS_2 — CAS_2 and $\text{MgO} \cdot \text{Al}_2\text{O}_3$ (MA)— $2 \text{CaO} \cdot \text{SiO}_2$ (C_2S)— $2 \text{CaO} \cdot \text{Al}_2\text{O}_3 \cdot \text{SiO}_2$ (C_2AS) were chosen as an example for the first case. The second case was represented by the system C_2AS — MA — CAS_2 . To demonstrate the last case, the system CaO (C)— Al_2O_3 (A)— SiO_2 (S) was chosen. For the sake of comparison, the experimentally determined phase diagrams were taken from the literature [12]. The required thermodynamic data were taken from [13, 14] and are listed in Table I. The temperature dependence of the enthalpy of fusion was neglected in these calculations. In all the cases no three-fold coordinated atoms were considered, i.e. $\alpha_{3,j} = 0$ for all j . It was further assumed that one half of the aluminium atoms present were in the tetrahedral coordination throughout the whole concentration region in question and the rest of the Al^{III} atoms had a higher coordination, obviously an octahedral one, and so did not participate in the polyanionic network formation ($\alpha_{4,j} = 0.5$ for $j\text{A} = \text{Al}$). It is obvious that $\alpha_{4,j} = 1$ for silicon and that for $j\text{A} = \text{Ca}, \text{Mg}, \text{Mn}$, $\alpha_{4,j} = 0$. A comparison between the calcula-

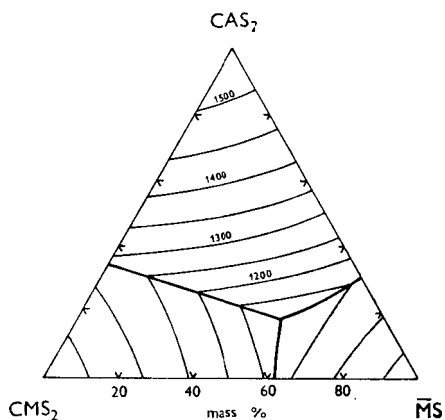


Fig. 4a. Calculated phase diagram of the CMS_2 — $\overline{\text{MS}}$ — CAS_2 system.

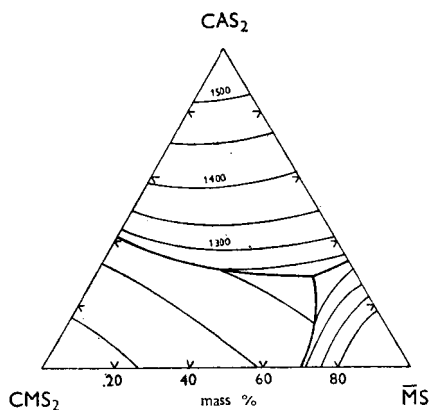


Fig. 4b. Experimental phase diagram of the CMS_2 — $\overline{\text{MS}}$ — CAS_2 system.

ted and experimentally determined phase diagrams is shown in Figs. 4a–8b. All the concentration data are in mass % and temperature is given in °C.

In Fig. 4a the calculated phase diagram of the CMS_2 – $\overline{\text{MS}}$ – CAS_2 system is shown. The experimental phase diagram [12] of the same system is shown in Fig. 4b. There is a discrepancy in the temperature of fusion of rhodonite, $\text{MnO} \cdot \text{SiO}_2$, given in [13] and in the experimental phase diagram [12]. The value of 1291 °C was used in the calculation.

A comparison of the calculated and experimental phase diagrams for the MS – CMS_2 – CAS_2 system is presented in Figs. 5a and 5b, respectively.

For the last example of the simple eutectic systems, the MA – C_2S – C_2AS system, the results of calculation and the experimental phase diagram are shown in Figs. 6a, 6b, respectively.

The systems with four crystallization areas, where the figurative point of the fourth crystalline phase lies outside the pseudoternary diagram, are represented by the C_2AS – MA – CAS_2 system (Figs. 7a, 7b). Because the enthalpy of fusion of MA has not been found in the calculation, this value was estimated on the basis

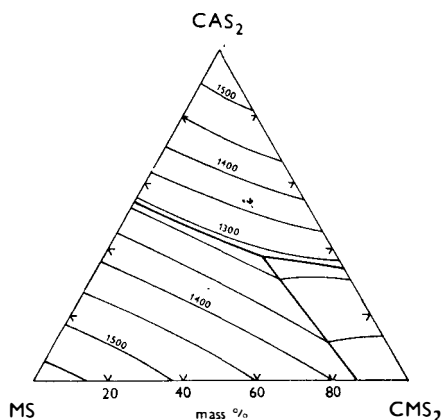


Fig. 5a. Calculated phase diagram of the MS – CMS_2 – CAS_2 system.

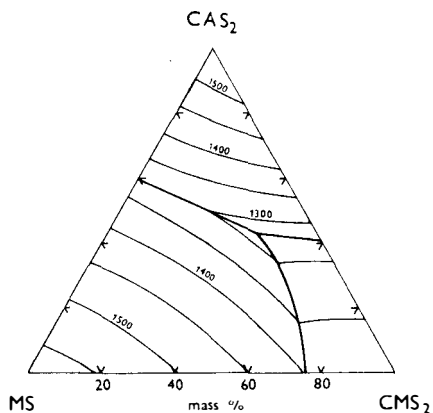


Fig. 5b. Experimental phase diagram of the MS – CMS_2 – CAS_2 system.

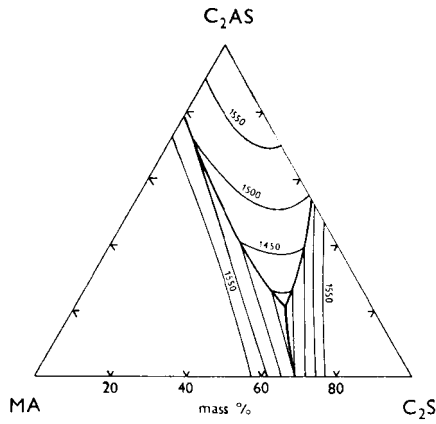


Fig. 6a. Calculated phase diagram of the MA—C₂S—C₂AS system.

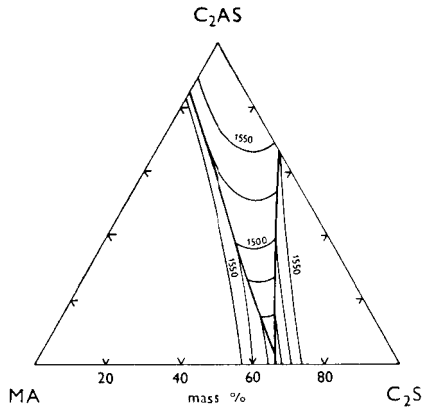


Fig. 6b. Experimental phase diagram of the MA—C₂S—C₂AS system.

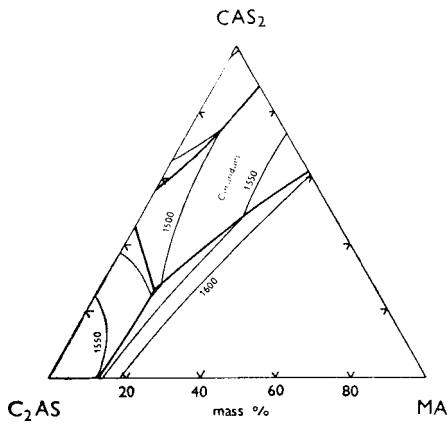


Fig. 7a. Calculated phase diagram of the C₂AS—MA—CAS₂ system.

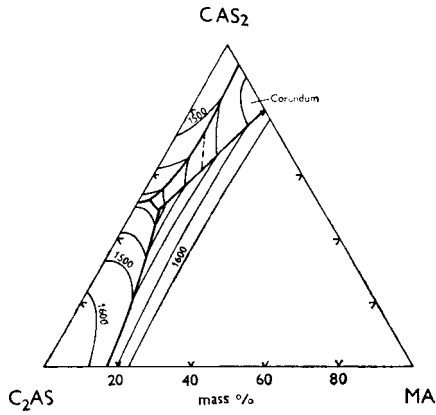


Fig. 7b. Experimental phase diagram of the C_2AS — MA — CAS_2 system.

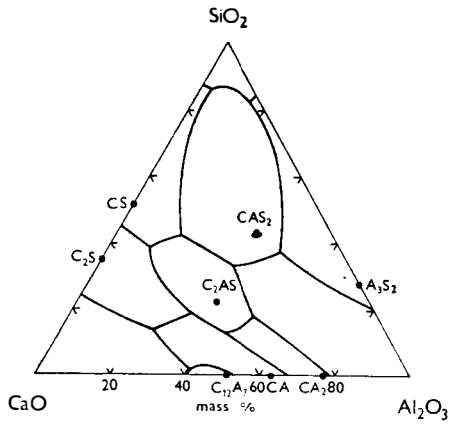


Fig. 8a. Calculated phase diagram of the C—A—S system.

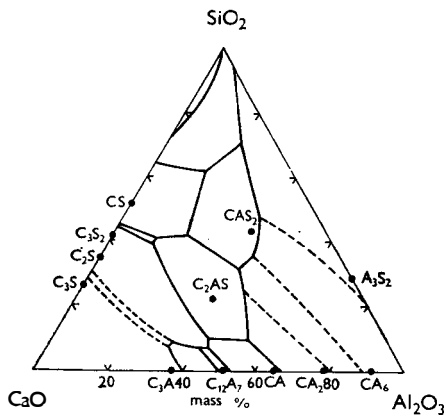


Fig. 8b. Experimental phase diagram of the C—A—S system.

of the thermodynamic analogy (the entropy of fusion is a sum of the entropies of fusion of the individual oxides).

The calculated and experimental phase diagrams of the C—A—S system, which represents the last type of the ternary systems considered, are shown in Figs. 8a and 8b respectively. In this case the immiscibility region near the SiO₂ apex was neglected in the solution since such behaviour is not considered in the thermodynamic model. Furthermore, because of lack of thermodynamic data, the crystallization of rankinite, tricalcium silicate, tricalcium aluminate and calcium hexaaluminate were not included in the calculation.

CONCLUSIONS

From the comparison of the calculated and experimental phase diagrams it follows that the computational procedure employed is suitable for describing the phase equilibrium in multicomponent silicate systems. Moreover, the introduction of some structural aspects into the thermodynamic model permits more information on the structure of the silicate melts to be obtained. Some disagreements in case of some calculated and experimental phase diagrams are obviously caused by either inadequate structural assumptions or unreliable thermodynamic data. More precise and correct values of the thermodynamic properties are therefore required. The practical significance of the calculation also lies in that it can be used in planned experiments, and thus reduce the number of tedious experimental measurements.

References

- [1] Spencer P. J., Barin I.: *Mater. Eng. Appl.* 1, 167 (1979).
- [2] Ansara I.: *Int. Met. Rev.* 24, 20 (1979).
- [3] Lukas H. L., Weiss J., Henig E.: *Th.: CALPHAD* 6, 229 (1982).
- [4] Kaufman L., Bernstein H.: *Computer Calculation of Phase Diagrams*. Acad. Press, New York and London 1970.
- [5] Horsák I., Sláma I.: *Chem. Papers* 41, 23 (1987).
- [6] Yiang Z., Hu X., Zhao X.: *J. Non-cryst. Solids* 52, 235 (1982).
- [7] Prigogine I.: *Bull. Soc. Chim. Belg.* 52, 115 (1943).
- [8] Pánek Z., Daněk V.: *Silikáty* 21, 97 (1977).
- [9] Daněk V., Pánek Z.: *Silikáty* 23, 1 (1979).
- [10] Daněk V.: *Chem. Papers* 38, 379 (1984).
- [11] Daněk V.: *Silikáty* 30, 97 (1986).
- [12] Levin E. M., Robbins E. R., McMurdie H. F.: *Phase Diagrams for Ceramists*. Amer. Ceram. Soc., Columbus, Ohio 1964 and Supplement 1969.
- [13] Barin I., Knacke O.: *Thermochemical Properties of Inorganic Substances*. Springer Verlag, Berlin — Heidelberg — New York — Düsseldorf 1973.
- [14] Bottinga Y., Richet P.: *Earth Planet. Sci. Lett.* 40, 382 (1978);

POČÍTAČOVÁ KONŠTRUKCIA FÁZOVÝCH DIAGRAMOV SILIKÁTOVÝCH SÚSTAV

Marek Liška, Vladimír Daněk

*Spoločné laboratórium CCHV SAV a Výskumného a vývojového ústavu sklárskeho,
912 50 Trenčín*

Ústav anorganickéj chémie CCHV SAV, 842 36 Bratislava

Na základe termodynamického modelu sa navrhol všeobecný algoritmus a zostrojil sa fortranový program na výpočet izobarických fázových diagramov polymérnych oxidových sústav.

Programové vybavenie umožňuje určiť teplotu primárnej kryštalizácie pre jednotlivý konfiguračný bod a konštrukciu fázových diagramov pre binárne a ternárne sústavy.

Použitie programu sa demonštrovalo na príkladoch jednoduchých ternárných eutektických systémov, ternárnom systéme so štyrmi kryštalickými fázami a na ternárnom systéme so vznikom viacerných binárných zlúčenín.

Navrhol sa spôsob využitia vypracovaného algoritmu pri skúmaní štruktúry silikátových tavenín.

Obr. 1. Bloková schéma programu FADR.

Obr. 2. Návüznosti jednotlivých podprogramov programu FADR.

Obr. 3. Kreslenie izoteriem v kosoštvorcovej sieti.

Obr. 4a. Vypočítaný fázový diagram sústavy $\text{CMS}_2\text{—}\overline{\text{MS}}\text{—}\text{CAS}_2$.

Obr. 4b. Experimentálny fázový diagram sústavy $\text{CMS}_2\text{—}\overline{\text{MS}}\text{—}\text{CAS}_2$.

Obr. 5a. Vypočítaný fázový diagram sústavy $\text{MS—CMS}_2\text{—}\text{CAS}_2$.

Obr. 5b. Experimentálny fázový diagram sústavy $\text{MS—CMS}_2\text{—}\text{CAS}_2$.

Obr. 6a. Vypočítaný fázový diagram sústavy $\text{MA—C}_2\text{S—C}_2\text{AS}$.

Obr. 6b. Experimentálny fázový diagram sústavy $\text{MA—C}_2\text{S—C}_2\text{AS}$.

Obr. 7a. Vypočítaný fázový diagram sústavy $\text{C}_2\text{AS—MA—CAS}_2$.

Obr. 7b. Experimentálny fázový diagram sústavy $\text{C}_2\text{AS—MA—CAS}_2$.

Obr. 8a. Vypočítaný fázový diagram sústavy C—A—S .

Obr. 8b. Experimentálny fázový diagram sústavy C—A—S .

КОНСТРУКЦИЯ ФАЗОВЫХ ДИАГРАММ СИЛИКАТНЫХ СИСТЕМ С ПОМОЩЬЮ ВЫЧИСЛИТЕЛЬНОЙ МАШИНЫ

Марек Лишка, Владимир Данек

*Общая лаборатория Центра химического исследования САН и Научно-исследовательского
и проектного института стекла, 912 50 Тренчин*

Институт неорганической химии

Центра химического исследования САН, 812 36 Братислава

На основании термодинамической модели авторами предлагается общий алгоритм и построение фортрановской программы, предназначенной для расчета изобарических фазовых диаграмм полимерных систем оксидов.

С помощью программы можно установить температуру первичной кристаллизации для отдельной точки конфигурации и конструкции фазовых диаграмм для бинарных и тернарных систем.

Использование программы показывается на примере отдельных тернарных эвтектических систем, тернарной системы с четырьмя кристаллическими фазами и на тернарной системе с образованием нескольких бинарных соединений.

Авторами предлагается способ использования разработанного алгоритма при исследовании структуры силикатных расплавов.

Рис. 1. Блок-схема программы FADR.

Рис. 2. Последовательность отдельных подпрограмм программы FADR.

Рис. 3. Изображение изотерм в ромбической сетке.

Рис. 4a. Расчитанная фазовая диаграмма системы $\text{CMS}_2\text{—}\overline{\text{MS}}\text{—}\text{CAS}_2$.

Рис. 4b. Экспериментальная фазовая диаграмма системы $\text{CMS}_2\text{—}\overline{\text{MS}}\text{—}\text{CAS}_2$.

Рис. 5a. Расчитанная фазовая диаграмма системы $\text{MS—CMS}_2\text{—}\text{CAS}_2$.

Рис. 5b. Экспериментальная газовая диаграмма системы $\text{MS—CMS}_2\text{—}\text{CAS}_2$.

Рис. 6a. Расчитанная фазовая диаграмма системы $\text{MA—C}_2\text{S—C}_2\text{AS}$.

Рис. 6b. Экспериментальная фазовая диаграмма системы $\text{MA—C}_2\text{S—C}_2\text{AS}$.

Рис. 7a. Расчитанная фазовая диаграмма системы $\text{C}_2\text{AS—MA—CAS}_2$.

Рис. 7b. Экспериментальная фазовая диаграмма системы $\text{C}_2\text{A—S—MA—CAS}_2$.

Рис. 8a. Расчитанная фазовая диаграмма системы C—A—S .

Рис. 8b. Экспериментальная фазовая диаграмма системы C—A—S .